

Mitigation of Inter-Carrier Interference Induced by Phase Noise and Residual Carrier Frequency Offset in CO-OFDM Systems

Xun Guan, Tianwai Bo, and Calvin Chun-Kit Chan

Department of Information Engineering
The Chinese University of Hong Kong, Shatin, N.T., Hong Kong
guanxun@ie.cuhk.edu.hk

Abstract—We propose and experimentally demonstrate a novel method to mitigate the inter-carrier interference (ICI) induced by laser phase noise in CO-OFDM systems. Numerical studies also show its capability of jointly mitigating phase noise and residual carrier frequency offset.

Keywords—inter-carrier interference; laser phase noise; residual carrier frequency offset

I. INTRODUCTION

Recently, coherent optical orthogonal frequency division multiplexing (CO-OFDM) has drawn great interest in optical fiber transmission, owing to its high spectrum efficiency, flexibility and tolerance to chromatic dispersion (CD) and polarization mode dispersion (PMD) [1]. The great advances in digital signal processing (DSP) technology have also enabled very-high-speed processing of the OFDM signals. However, CO-OFDM systems are sensitive to laser phase noise (PN), which degrades the system performance in a two-fold manner, known as common phase error (CPE) and inter-carrier interference (ICI). In addition, CO-OFDM systems also suffer from the possible carrier frequency offset (CFO) between the transmitter laser and the receiver laser in the intradyne or heterodyne coherent receiving process. Even though designated DSP algorithms can be applied to estimate and compensate the CFO at the coherent receiver, there always exists Gaussian-distributed residual carrier frequency offset (RFO) that deteriorates the system performance [2]. Previous studies have unveiled that RFO also influenced the CO-OFDM system in the form of ICI [3].

In this paper, we present and experimentally demonstrate a method for mitigating the deteriorative ICI caused by PN. We also numerically demonstrate that the proposed algorithm can also reduce the ICI caused by PN and the RFO, simultaneously.

II. PRINCIPLES OF OPERATION

Suppose the complex baseband OFDM signal generated at the transmitter is represented as

$$x(t) = \sum_{m=0}^{N-1} S(m) \cdot e^{j2\pi f_m t}, \text{ for } 0 < t < T_s, f_m = \frac{m}{T_s} \quad (1)$$

where $S(m)$ and f_m are the data and the carrier frequency of the m^{th} subcarrier, respectively. For simplicity of discussion, other effects such as channel response are neglected. After sampling at the coherent receiver, the received signal in time domain can be expressed in discrete form as

$$\begin{aligned} r(n) &= x(n) \cdot e^{j\theta(n)} + \eta \\ &= e^{j\theta(n)} \cdot \sum_{m=0}^{N-1} S(m) \cdot e^{j2\pi f_m n} + \eta \end{aligned} \quad (2)$$

where $\theta(n)$ is the phase variation caused by PN and CFO. η is the white Gaussian noise. The recovered k^{th} subcarrier after the fast Fourier transform (FFT) can be expressed as

$$\begin{aligned} \hat{S}(k) &= \frac{1}{N} \sum_{n=0}^{N-1} r(n) e^{-j2\pi f_k n} \\ &= \frac{1}{N} \sum_{n=0}^{N-1} e^{j\theta(n)} \cdot \sum_{m=0}^{N-1} S(m) \cdot e^{j2\pi(f_m - f_k)n} + \eta' \\ &= \sum_{k=0}^{N-1} S(m) \cdot I(m-k) + \eta' \end{aligned} \quad (3)$$

$$I(i) = \frac{1}{N} \sum_{n=0}^{N-1} e^{j2\pi n f_i} \cdot e^{j\theta(n)}, \quad f_i = \frac{i}{N} \quad (4)$$

where the symbol η' is the complex Gaussian noise sample term. The sequence $I(i)$ is the ICI coefficients. Rewrite (3) as

$$\hat{S}(k) = S(k) \cdot I(0) + \sum_{k=1}^{N-1} S(m) \cdot I(m-k) + \eta' \quad (5)$$

The second term in (5) is the ICI term, contributed by all the other subcarriers in the OFDM symbol. The involvement of excessive subcarriers would lead to prohibitively difficult in ICI mitigation. However, PN is usually modelled as a Wiener process with a low-pass Gaussian distributed power spectral density (PSD) [4,5]. On the other hand, the ICI induced by CFO also has low-pass property [3]. Hence, only several neighboring subcarriers around $S(k)$ are dominant. Therefore, $\hat{S}(k)$ can be seen as a weighted sum of several pairs of localized subcarriers. After the multiplicative coefficients are estimated, ICI can be compensated by DSP.

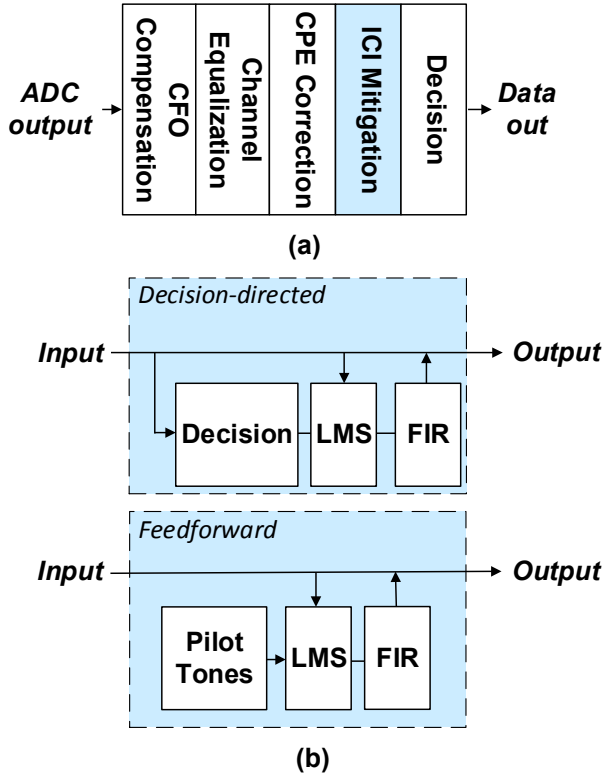


Fig. 1. (a) DSP process, (b) ICI mitigation process

The above discussions pave the way for the mitigation of ICI. Fig. 1(a) shows the equalization process at the CO-OFDM receiver side (inverse FFT (IFFT) and cyclic prefix (CP) removal are not shown). An ICI mitigation step can be added after CPE correction. The estimation of the filter coefficients here is based on least-mean-square (LMS) method. Fig 1(b) shows the process of two algorithms of DSP filter coefficients estimation, i.e., decision-feedback (DF) [6] and feed-forward (FF) [4]. In DF, only a small number of pilots are needed to compensate the CPE for the tentative decision of the other subcarriers, which are then used for the filter coefficients estimation. The justification of using this DF algorithm is that only a small portion of the tentative decided symbols are erroneous [6]. Instead, more pilots are necessary in FF algorithm so as to achieve a comparable performance as DF. The sacrifice of transmission rate of FF reduces the computing complexity, compared to DF, since no decision-feedback is required. Moreover, the ICI mitigation step in DF can also function as CPE corrector, hence removing the CPE correction step before ICI mitigation. In this paper, we only use a 3-tap FIR filter for ICI mitigation. Only the interference induced by a pair of adjacent subcarriers is considered as aforementioned.

III. EXPERIMENTS

Experiments have been conducted to verify the effectiveness of the proposed scheme in mitigating ICI induced by PN. Fig. 2 depicts the experimental setup. The output of an external cavity laser (ECL) was modulated by an optical I-Q modulator, driven by the electrical signal from a Tektronix arbitrary waveform generator (AWG), operating at 12 Gsample/s. The OFDM

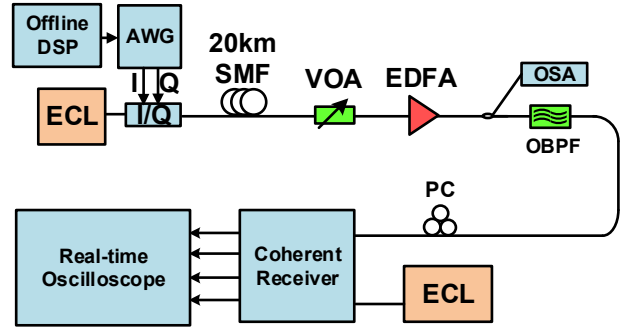


Fig. 2. Experimental setup

waveform was generated offline in MATLAB in a FFT size of 256, of which 128 was modulated with quadrature phase-shift keying (QPSK) data. A CP of 32 samples was added. Each OFDM symbol comprised 20 training symbols as the channel estimator and 512 data symbols. The OFDM data in the time domain after IFFT was then multiplied by a sequence of digitally generated random complex number so as to emulate the effect of PN [7]. The number sequence was specially designed, according to the model of PN.

The modulated signal was then fed into a piece of 20-km single mode fiber (SMF). A variable optical attenuator (VOA), followed by an Erbium doped fibre amplifier (EDFA) were used to control the signal power and the optical signal-to-noise ratio (OSNR). A portion of the signal was then split off to an optical spectrum analyser (OSA) to monitor the OSNR, while the rest of the signal was fed into an optical coherent receiver for detection. A 0.88-nm bandwidth optical bandpass filter was inserted to filter out the out-of-band noise at the coherent receiver. A polarization controller was placed before the coherent receiver to align the input signal to only one polarization of the coherent receiver. The output of the coherent receiver was captured with a digital sampling analyser (DSA) and was offline processed under MATLAB. The number of pilot

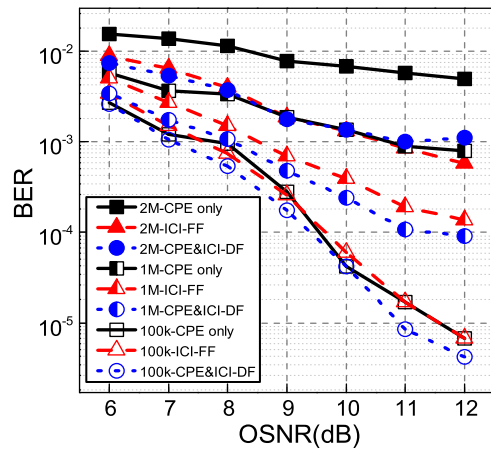


Fig. 3. Experimental results (legend: laser linewidth in Hz-DSP algorithm-DF or FF).

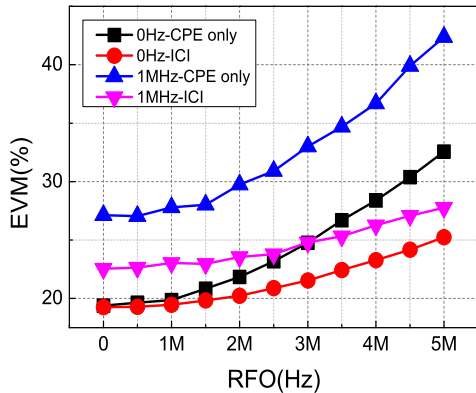


Fig. 4. Simulation results (legend: laser linewidth -DSP algorithm).

tones for ICI mitigation in FF algorithms was set to be 24, while in the case of DF, 8 subcarriers were used as pilot tones for CPE correction, prior to tentative decisions. The BER was calculated by counting the number of errors over 5000 data symbols.

IV. EXPERIMENTAL RESULTS AND DISCUSSIONS

Fig. 3 shows the experimental results of PN mitigation under difference OSNR values, different laser linewidths (100 kHz, 1 MHz, 2 MHz), and different ICI mitigation schemes (ICI-DF, ICI-FF). The results were compared to that with only CPE correction. It could be seen that when the 3-dB laser linewidth was 100 kHz, the ICI mitigation algorithm achieved nearly no obvious improvement in BER performance. However, when the laser linewidth was increased to 1 MHz, the performance improvement was quite obvious. The required OSNR at $\text{BER}=10^{-3}$ was reduced by about 3 dB. When the laser linewidth was 2 MHz, the BER performance without PN mitigation even could not reach the level of 10^{-3} , while the OSNR requirement to reach this threshold was 12 dB. Therefore, the proposed method was remarkably effective in mitigating the PN. On the other hand, the performances of the ICI mitigation schemes using DF and FF were almost the same.

V. SIMULATION RESULTS AND DISCUSSIONS

We have also simulated the performance of the proposed algorithm in jointly combatting the ICI induced by RFO and PN. The setup for the emulative study was the same as that in the experiment. The OSNR was fixed at 8 dB. The ICI mitigation scheme adopted was FF, which saved CPE estimation in DSP. Hence the comparison of DSP algorithms was between the cases of only CPE correction and only ICI mitigation. The laser

linewidth was set to be 1 MHz, as well as 0 Hz (i.e., ideal single tone laser), as the benchmark of merely RFO mitigation, respectively. The RFO was varied from 0 to 5 MHz (negative RFOs were neglected due to the symmetry of the EVM performance). Fig. 4 depicts the EVM values of the given linewidth and RFO under difference DSP algorithms.

When the laser linewidth was set at 0 Hz, the differences of the EVM values between the cases with and without ICI mitigation proved that the proposed ICI mitigation method could sufficiently compensate the ICI induced by RFO. When the laser linewidth was 1 MHz without ICI mitigation, the EVM deteriorated drastically when RFO increased. With the help of ICI mitigation, EVM could be largely reduced, indicating a remarkable mitigation of ICI induced by RFO. Specially, when the case laser linewidth was 1 MHz and RFO was 0 Hz, the 5% decrease of EVM achieved by ICI mitigation should be attributed to the mitigation of PN. When the RFO was 3 MHz with no PN, the EVM reduction brought by RFO compensation only was 3%. The ICI mitigation algorithm could reduce the EVM by about 8% in case of 3-MHz RFO and 1-MHz linewidth, indicating that the ICI induced by PN and RFO were simultaneously mitigated.

VI. SUMMARY

We have proposed and experimentally demonstrated a new ICI mitigation method, which can mitigate the performance penalty caused by laser phase noise. It is further showed that when there exists residual carrier frequency offset, the ICI caused by PN and RFO can be simultaneously mitigated.

REFERENCES

- [1] W. Shieh, H. Bao, and Y. Tang, "Coherent optical OFDM: theory and design," *Optics Express*, Vol. 16, no. 2, pp. 841-859, 2008.
- [2] J. Zhao, and A. Ellis, "Advantage of optical fast OFDM over OFDM in residual frequency offset compensation," *Photon. Technol. Lett.*, vol. 24, no.24, pp. 2284-2287, 2012.
- [3] T. Kanesan, S. T. Le, D. Roque, and A. Ellis, "Non-rectangular perfect reconstruction pulse shaping based ICI reduction in CO-OFDM," *Optics Express*, vol. 22, no. 2, pp.1749-1759, 2014.
- [4] M. R. Gholami, Said Nader-Esfahani, and A. A. Eftekhar, "A new method of phase noise compensation in OFDM," *Proc. ICC*, vol. 5, pp. 3443-3446, 2003.
- [5] E. Ip, and Joseph M. Kahn, "Feedforward carrier recovery for coherent optical communications," *J. Lightwave Technol.*, vol. 25, no. 9, pp. 2675-2692, 2007.
- [6] D. Petrovic, W. Rave, and G. Fettweis, "Phase noise suppression in OFDM including intercarrier interference," *Proc. Intl. OFDM Workshop (InOWo)*, vol. 3, pp. 219-224, 2003.
- [7] Z. Zan, and A. J. Lowery, "Experimental demonstration of a flexible and stable semiconductor laser linewidth emulator," *Optics Express*, vol. 18, no. 13, pp. 13880-13885, 2010.